ISIJ International, Vol. 60 (2020), No. 10, pp. 2255–2265
https://doi.org/10.2355/isijinternational.ISIJINT-2020-086

Newly Developed Wear Testing Machine Having Sufficient Reproducibility Useful for Investigating Roller Chains

Ryoichi SAITO,[1)]* Nao-Aki NODA[2)] and Yoshikazu SANO[2)]

1) Senqcia Corporation Kanto Works, 5100 Mikajiri, Kumagaya-shi, Saitama-ken, 360-0843 Japan.
2) Dept. of Mechanical and Control Engineering, Kyushu Institute of Technology, 1-1 Sensui-cho Tobata-ku, Kitakyushu-shi, Fukuoka, 804-8550 Japan.

(*Received on February 25, 2020; accepted on April 10, 2020; originally published in Tetsu-to-Hagané, Vol. 106, 2020, No. 1, pp. 28–38*)

Roller chains are commonly used to transmit mechanical power in many kinds of machineries for wide industrial fields. Roller chain manufactures are doing a lot of efforts to improve the wear resistance through conventional real chain type wear testing with huge amount of time and cost. In this study, a new wear testing machine is developed to evaluate wear amounts more efficiently without using main chain components such as inner plate, outer plate and roller. The results show that the nearly same amounts of wear rate and wear status can be obtained between the newly developed wear testing machine and the conventional machine. It may be concluded that the newly developed wear testing has sufficient reproducibility and can be used more conveniently for investing roller chains compared to the conventional wear testing machine.

KEY WORDS: roller chain; wear; testing machine; pin; bush.

1. Introduction

Roller chains are commonly used to transmit mechanical power in many kinds of industrial machineries including conveyors, motorcycles, bicycles, and so forth. The driving force is directly transmitted to the chain by the engaged sprocket, which is connected to a power source. Compared with the belt drive, the transmission capacity is much larger, the slip is negligibly smaller, and the transmission efficiency is higher. The life of the roller chain is usually determined by the chain elongation except sudden breakage of the link-plate or pin. When the chain engages with the sprocket, the outside diameter of pin and the inside diameter of bush are gradually wearing out by the sliding motion each other. This wear causes the chain elongation causing the improper engaging with sprocket. Therefore, roller chain manufactures are doing a lot of efforts to improve the wear resistance.[1–11)]

The wear resistance is now being evaluated by using the conventional chain type wear testing machine consisting of real chains and sprockets. However, huge amounts of time and cost are necessary for preparing and installing real chains and sprockets even before testing. In the previous study, therefore, simplified testing machine composed by a few members of outer links and inner links was studied;[12,13)] however, the diameter profile of the pin after testing was different from of the real chain profile and the accuracy was not discussed.

In recent years, high-performance materials such as ceramics are being partly used in roller chain. Such new roller chains are planned to be used in the heating furnace where high wear resistance is required.[14)] However, since such ceramics components are expensive and difficult to be manufactured, the conventional chain type wear testing machine hardly be applied. This study focuses on developing a new wear testing machine to evaluate such wear amount conveniently.

2. Wear of Real Roller Chain and Evaluation Method

2.1. Conventional Wear Testing Machine for Real Roller Chain

Figure 1 shows the schematic illustration of the roller chain including five components. Here, notation T denotes the magnitude of tensile load during operation. The bush and the pin are pressed into the inner plate and the outer plate so that they cannot rotate but only the roller can rotate around the bush. The outer link consists of the pin and the outer plate as shown ① in Fig. 1. The inner link consists of the bush and the inner plate as shown ② in Fig. 1. The wear occurs between the pin and the bush due to sliding under tensile load condition, and the wear amount increases

* Corresponding author: E-mail: Ryoichi.Saito@senqcia.com

© 2020 The Iron and Steel Institute of Japan. This is an open access article under the terms of the Creative Commons Attribution-NonCommercial-NoDerivs license (https://creativecommons.org/licenses/by-nc-nd/4.0/).

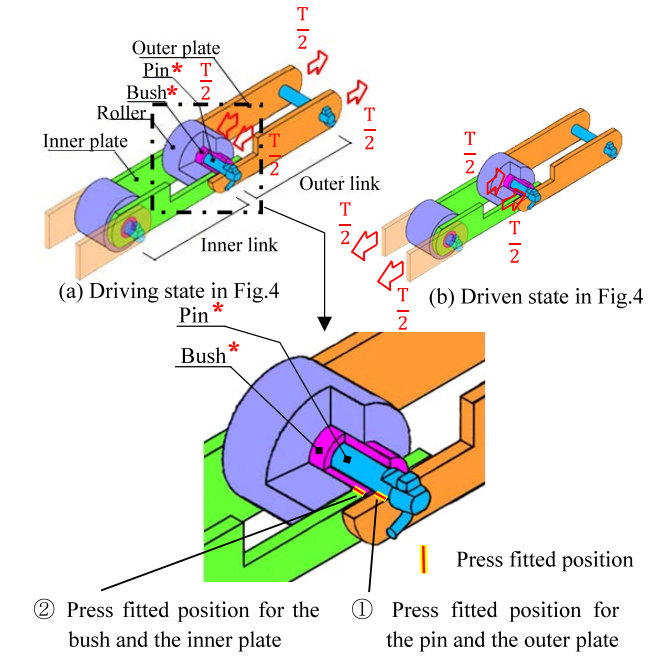

Fig. 1. Schematic illustration of the roller chain whose mechanical wear between the pin and the bush causes elongation and final failure. (Online version in color.)

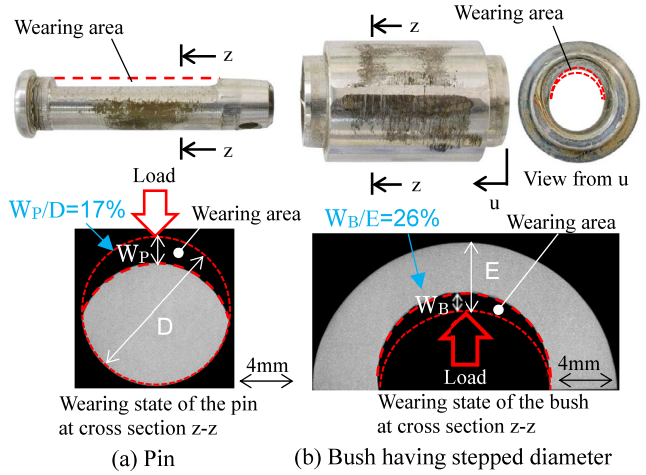

Fig. 2. Pin and bush whose wear amounts reach the use limit. (Online version in color.)

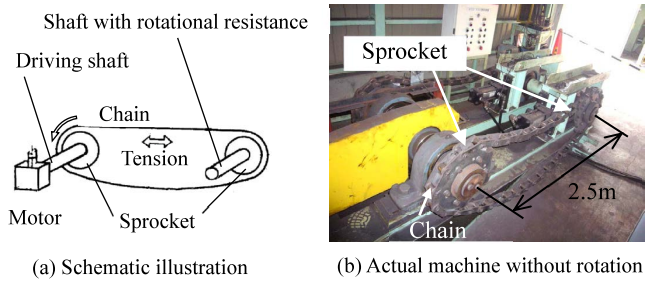

Fig. 3. Conventional chain type wear testing machine for the roller chain. (Online version in color.)

during the use. **Figure 2** shows examples of roller chain components that cannot be used anymore because the chain elongation is over 2% after real operation. In general, 2% chain elongation is used as the allowable limit. Figure 2(a) shows the pin whose wear depth W_P is about 17% of the outer pin diameter. Figure 2(b) shows the bush whose wear depth W_B is about 26% of the bush thickness. The wear amount $W_T=W_P+W_B$ corresponds to the chain elongation.

Figure 3 shows the conventional chain type wear testing machine.[15] Since this testing machine consists of real chain components and sprockets, the results can be regarded as the real use results.[15] However, this testing needs a huge amount of time and cost just for preparing and installing the real chains and sprockets. Therefore, this study focuses on developing a new wear testing machine, which can evaluate the wear amount efficiently without using main chain components such as inner plate, outer plate and roller, and has sufficient reproducibility useful for investigating roller chains.

2.2. Wear Mechanism of the Real Roller Chain

2.2.1. Why Wear Occurs in the Real Roller Chain during Operation

Figure 4 shows illustrates the range A, B, C, D, E, F, each of which has distinct mechanical state in the real roller chain. **Table 1** shows the variation of the tensile load and the variation of the bend angle. The roller chain wear by the changed bend angle during the tensile load is caused. Table 1 shows the bend angle changes under the tensile load in ranges A and B. In other ranges, there is no angle change. Therefore, the wear occurs only in the range A and B. In this paper, the driving state is defined as range A as shown in Fig. 4 and the driven state is defined as range B as shown in Fig. 4.

Here, the bend angle θ_A change occurs due to the sprocket rotation. As shown in the range A in Fig. 4, if θ_A is defined as $\theta_A=\angle OAO'$, then we have $0\leq\theta_A\leq\theta_0$ under tension T. Here, the angle θ_0 specifies the interval of sprocket teeth as $\theta_0=2\pi/N$, where N is the number of teeth in the sprocket. When the pin and bush are at the position A_1 (see the black point in Fig. 4), the bend angle $\theta_A=\theta_0$. When the black point in Fig. 4 moves to the position A_2, the bend angle change from $\theta_A=0$ to $\theta_A=\theta_0$ occurs due to sprocket rotation. Since the pin is fixed to the outer plate and the bush is fixed to the inner plate, the bend angle of the outer plate and the inner plate is equal to the angle between the pin and the bush. Since an angle change from $\theta_A=0$ to $\theta_A=\theta_0$ occurs between the pin and the bush under the tensile load, the friction and wear occur in the range A in Fig. 4.

The frictional situation of the range B is the same as the range A. If θ_B is defined as $\theta_B=\angle OBO'$, then we have $0\leq\theta_B\leq\theta_0$ under tension T. When the pin and bush are at the position B_1 (see the black point in Fig. 4), the bend angle $\theta_B=\theta_0$.When the black point in Fig. 4 moves to the position B_2, the bend angle change from $\theta_B=\theta_0$ to $\theta_B=0$ occurs due to sprocket rotation. Since an angle change from $\theta_B=\theta_0$ to $\theta_B=0$ occurs between the pin and bush under the tensile load, the friction and wear occur in the range B in Fig. 4.

2.2.2. Sliding State of the Pin and the Bush

Figure 5 shows the sliding states of the pin and bush in the range A and range B in Fig. 4 where the wear is caused as explained in the previous section. Note that Fig. 5 shows the case where the teeth of sprocket enter the outer link, and the roller is not drawn in the figure. Figure 5(a) shows the

© 2020 ISIJ

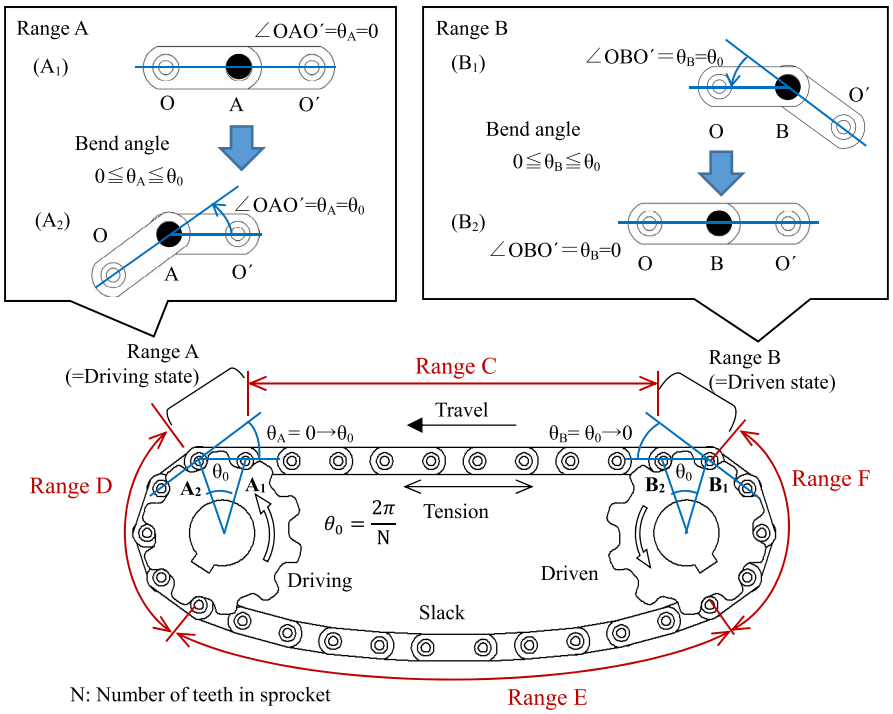

Fig. 4. Illustration for the range A, B, C, D, E, F, each of which has distinct mechanical state in the roller chain. (Online version in color.)

Table 1. Variation of tensile load and bend angle.

Range	Tensile load	Bend angle	Wear
A	T	Changing as $\theta_A=0\rightarrow\theta_0$	Appears
B	T	Changing as $\theta_B=\theta_0\rightarrow0$	Appears
C	T	Fixed as $\theta_C=0$	Not appears
D	T→0	Fixed as $\theta_D=\theta_0$	Not appears
E	0	$\theta_E\fallingdotseq0$ Depending on the slack of the chain	Not appears
F	0→T	Fixed as $\theta_F=\theta_0$	Not appears

Table 2. Definition of position A_1, A_2, B_1, B_2 and θ_0 in range A, B shown in Fig. 4.

Items	Definition
Position A_1	The chain starts engaging with the sprocket under tension in the driving side.
Position A_2	The chain is bent at angle θ_0 under tension in the driving side.
Position B_1	The chain starts to move away from the sprocket under tension in the driven side.
Position B_2	The chain is bent at angle θ_0 under tension in the driven side.
Angle θ_0	The angle specifies the interval of sprocket teeth as $\theta_0=\frac{2\pi}{N}$, where N is the number of teeth in sprocket

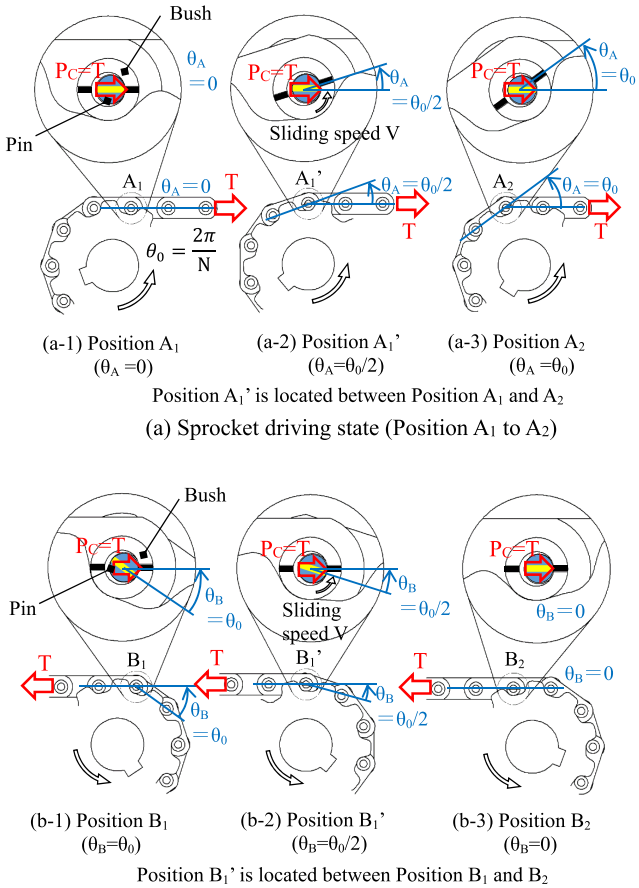

Fig. 5. Load and sliding condition of the driving state and the driven state. (Online version in color.)

range A of Fig. 4, and Fig. 5(b) shows the range B of Fig. 4.

First, the sliding between the pin and the bush in the driving state is explained. Figure 5(a-1) illustrates geometrical condition of the position A_1 in Fig. 4, and the bend angle $\theta_A=0$. Figure 5(a-3) illustrates geometrical condition of the position A_2 in Fig. 4, and the bend angle $\theta_A=\theta_0$. Figure 5(a-2) shows the position of the bend angle $\theta_A=\theta_0/2$. In the driving state, the contact load Pc = T occurred between the pin and the bush by the tensile load of the chain. As shown

© 2020 ISIJ

in Fig. 5(a-2), the bush rotates counterclockwise under the compressive state due to the sprocket's rotation. The rotation of the bush stops at an angle θ_0 as shown in Fig. 5(a-3). Here, sliding speed V is circumferential speed of the inner surface of the bush. As shown in Fig. 5(a), in the driving state, the pin is fixed under the compressive state of the contact load Pc = T, and the bush rotates from $\theta_A=0$ to $\theta_A=\theta_0$ at the sliding speed V.

Next, the sliding between the pin and the bush in the driven state is explained. Figure 5(b-1) illustrates geometrical condition of the position B_1 in Fig. 4, and the bend angle $\theta_B=\theta_0$. Figure 5(b-3) illustrates geometrical condition of the position B_2 in Fig. 4, and the bend angle $\theta_B=0$. Figure 5(b-2) shows the position of the bend angle $\theta_B=\theta_0/2$. In the driven state, the contact load Pc = T occurred between the pin and the bush by the tensile load of the chain. As shown in Fig. 5(b-2), the pin rotates counterclockwise under the compressive state due to the sprocket's rotation. The rotation of the pin stops at an angle θ_0 as shown in Fig. 5(b-3). As shown in Fig. 5(b), in the driven state, the bush is fixed under the compressive state of the contact load Pc = T, and the pin rotates from $\theta_A=0$ to $\theta_A=\theta_0$ at the sliding speed V.

As shown in Fig. 5, wear mechanism is clarified in the real roller chain during operation. The wear of the roller chain occurs when the bend angle is changed under the tensile load. In the driving state, the pin is fixed under the compressive state, and the bush rotates. In the driven state, the bush is fixed under the compressive state, and the pin rotates.

3. The Newly Developed Wear Testing Machine Having Sufficient Reproducibility of the Real Sliding State between the Pin and the Bush

3.1. How to Design the Newly Developed Wear Testing Machine

Since the conventional chain type wear testing machine consists of real chain components and sprockets, the results can be regarded as the real use results. However, such testing machine needs a huge amount of time and cost to prepare for the real chains and sprockets. Therefore, we set up the following principles 1) and 2) for designing the newly developed wear testing machine.

The design principle 1) is to have sufficient reproducibility of the actual sliding state of the pin and the bush in the real roller chain.

The design principle 2) is to be composed by minimum components in order to simplify the testing machine.

According to the design principle 1), the newly developed wear testing machine may obtain the similar wear rate composed to the conventional chain type wear testing machine. However, the wear results of the conventional chain type wear testing machine sometimes have larger scatter because of the vibration when the chain engages with the sprocket, manufacturing tolerances of the components, and errors due to the assembly and installation. Therefore, according to the design principle 2), the newly developed machine consists of just a pin and a bush as shown in **Figs. 7** and **8** to improve the reproducibility, to reduce the cost of the test pieces and to reduce the preparing time. The pin and the bush used in the new testing machine have almost the same dimensions of the real roller chains.

3.2. Reproductive Mechanism for the Wear of Pin and Bush

Figure 6 illustrates the sliding direction at the surface of the pin and bush for the newly developed wear testing in comparison with the real chain. To realize the sufficient reproducibility, in the newly developed wear testing machine, the pin is fixed and the bush slides reciprocatively. As shown in Figs. 5 and 6, wear mechanism is clarified in the real roller chain during operation. In the driving state, the pin is fixed under the compressive state, and the bush rotates. In the driven state, the bush is fixed under the compressive state, and the pin rotates. In Fig. 6, it should be noted that the chain elongation in the real roller chain is caused by the wear at point P and point Q. And the wear is caused by the reciprocating motion at those points.

To simplify the friction state of the real roller chain, in the newly developed wear testing machine, the pin is fixed under constant load and the bush slides reciprocatively. During the operation, the sliding motions of point P and point Q are reciprocating. Since the sliding direction during the operation is the same as the sliding direction of the real roller chain, the newly developed wear testing machine adopts such reciprocating motions. Moreover since those frictional motion is easy to be controlled, the newly developed wear testing machine may improve the test accuracy to reduce the errors due to the assembly and installation. The detailed explanation of the sliding direction is shown in the appendix.

3.3. Schematic Illustration of Sliding Component for the Newly Developed Wear Testing Machine

Figure 7 shows the schematic illustration of the newly developed wear testing machine. The bush of the test piece is press-fitted into the holder. The holder, jig A and jig B are assembled to integrate. As shown in Fig. 7(b), the pin is inserted into the interior of the bush. Motor shaft is connected directly to jig A to slide the bush. As shown in Fig. 7(b), both ends of the pin protruding from the end surface of

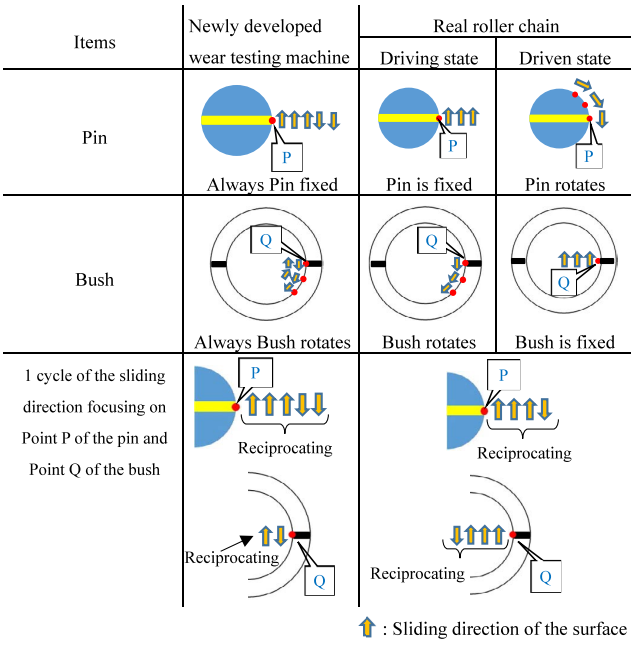

Fig. 6. Comparison of the sliding direction of the surface. (Online version in color.)

© 2020 ISIJ

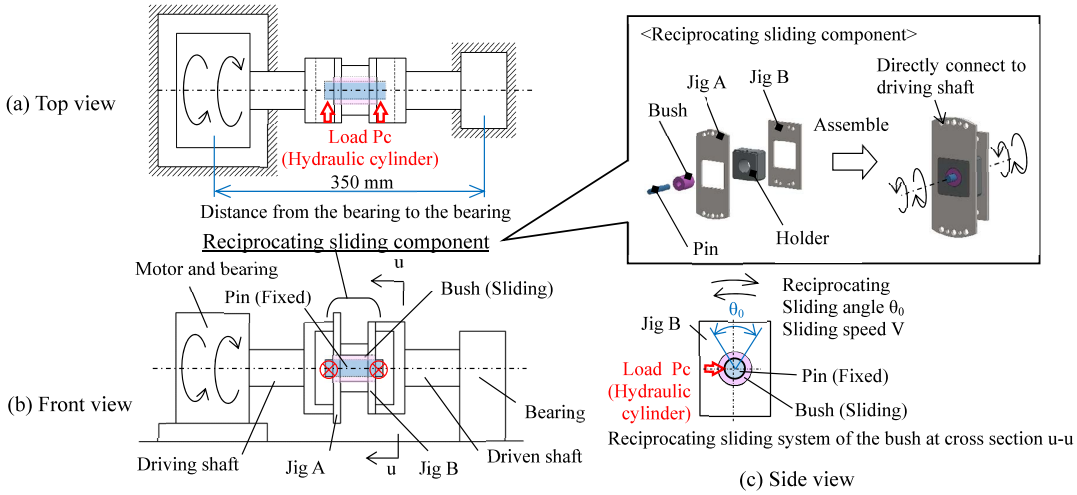

Fig. 7. Schematic illustration of the newly developed wear testing machine. (Online version in color.)

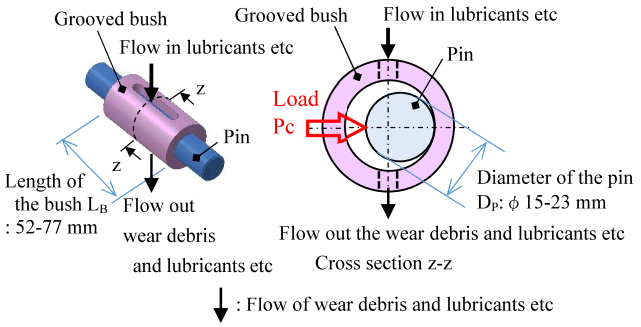

Fig. 8. Grooved bush to remove the wear debris and lubricants. (Online version in color.)

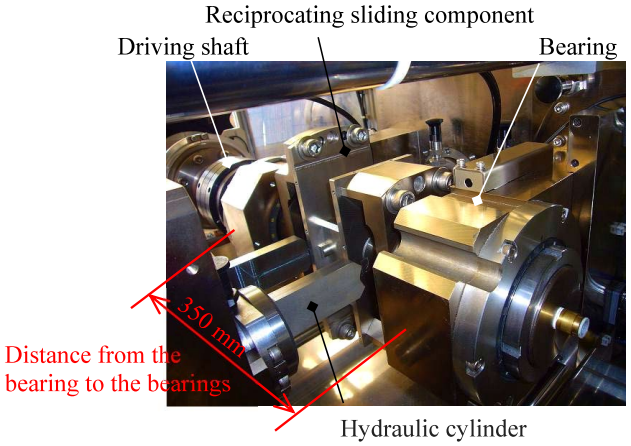

Fig. 9. Photograph of the newly developed wear testing machine. (Online version in color.)

the bush are pressed horizontally by the hydraulic cylinder not to rotate the pin. Then the motor is operated reciprocatively under the fixed pin condition to slide the bush reciprocatively. The hydraulic cylinder moves horizontally to keep the constant pressure between the pin and the bush even when the pin and the bush are worn out. The total amount of wear between the pin and the bush can be measured without removing the pin and the bush from the testing machine by the displacement amount of the hydraulic cylinder. Figure 8 shows the grooved bush to remove the wear debris and lubricants. Compared to the real roller chain, in the newly developed wear testing machine, the wear debris accumulate easily because of less vibrations. The grooved bush in the vertical direction can remove this debris by applying holizontal loading.

3.4. Specification of the Newly Developed Wear Testing Machine

Figure 9 shows the appearance of the reciprocating sliding component for the newly developed wear testing machine. This testing machine can evaluate the pin diameter in the range D_P = 15 mm–23 mm. In the future, another type new testing machine is planned to be developed to evaluate the pin diameter in the range D_P = 10 mm–100 mm by using the same structure. **Table 3** shows the specification of the newly developed wear testing machine.

Table 3. Specification of the newly developed wear testing machine.

Whole size		1 700×1 300×1 800 [mm]
Load	Pc	700–80 000 [N]
Average sliding speed	V	0.01–7 [m/min]
Idling time		0.01–9.99 [sec]
Sliding angle	θ_0	0.2–72 [degree]
Diameter of the pin	D_P	ϕ 15–23 [mm]
Diameter of the bush	D_B	ϕ 22–40 [mm]
Inside diameter of the bush	D_{BI}	ϕ 16–24 [mm]
Length of the pin	L_P	68–100 [mm]
Length of the bush	L_B	52–77 [mm]
Length of the sliding area		52–77 [mm]

4. Comparison of the Results between the Newly Developed Wear Testing and the Conventional Chain Type Wear Testing

4.1. Specification of Specimens and Testing Condition

Between the newly developed wear testing and the

© 2020 ISIJ

conventional chain type wear testing, the same conditions are assumed for specimen dimensions, loading and sliding speed. **Figure 10** shows the specimen dimensions where the pin outer diameter D_P = 15.8 mm, bush inner diameter D_{BI} = 16.3 mm, bush length L_B = 52.9 mm. The pin material is SCM435, and the bush material is SCM415. **Table 4** shows each chemical components of specimens. **Table 5** shows material properties and fabrication processes. For the newly developed wear testing machine, the pin and the bush are manufactured by lathe turning. For conventional chain type wear testing machine, however, the pin is manufactured by cold forging and the bush is manufactured by cold–drawn pipe. Therefore, it should be noted that the specimen has different surface properties due to distinct fabrication processes.

Figures 11 and **12** illustrate the difference in surface properties. Figure 11 shows an axial cross section of near surface of the pin and the bush for the newly developed wear testing. As shown in Figs. 11(a-2) and 11(b-2), at the near surface, lathe turning marks are observed without the oxide film. It should be noted that at an axial cross section of the pin a remarkable rolling flow is observed in Fig. 11(a-1). Figure 12 shows an axial cross section of near surface of the pin and the bush for the conventional chain type wear testing. As shown in Figs. 12(a-2) and 12(b-2), an oxide film with about 20 μm thickness can be observed at the near surface. Those differences of the surface properties contribute initial wear difference as described in section 5.1.

Table 6 shows the testing condition. For real roller chains, lubricants such as oil to the sliding surface is recommended to improve the wear resistance. However, in this study, to

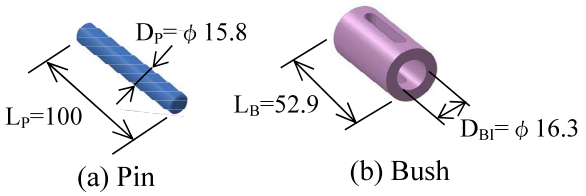

Fig. 10. Size of the pin and the bush for wear testing [mm]. (Online version in color.)

Table 4. Chemical composition of specimens [%].

Testing machine	Newly developed wear testing		Conventional chain type testing	
Items	Pin	Bush	Pin	Bush
Material	SCM435	SCM415	SCM435	SCM415
C	0.37	0.17	0.35	0.15
Si	0.26	0.30	0.19	0.21
Mn	0.81	0.78	0.76	0.76
P	0.023	0.016	0.014	0.013
S	0.023	0.012	0.020	0.013
Cr	1.11	0.90	1.12	0.98
Mo	0.15	0.15	0.16	0.18

Table 5. Surface properties of the pin and the bush.

Testing machine	Newly developed wear testing		Conventional chain type wear testing	
Items	Pin	Bush	Pin	Bush
Hardness [HRC]	55.4	59.1	55.0	59.6
Surface roughness Ry [μm]	6.4	12.0	13.6	5.4
Fabrication process	Lathe turning →Heat-treatment →Shotblasting		Cold forging →Heat-treatment →Shotblasting	Cold-drawn pipe →Heat-treatment →Shotblasting

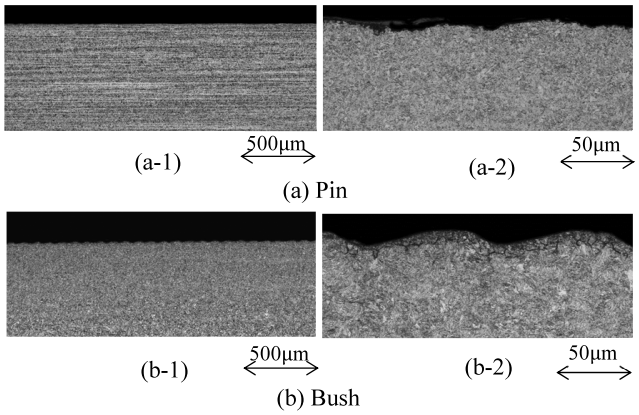

Fig. 11. Axial cross section of the near surface of the pin and the bush used for the newly developed wear testing (5% Nital etching).

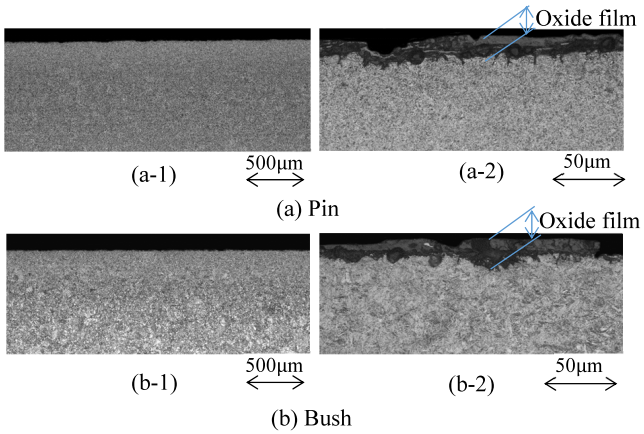

Fig. 12. Axial cross section of the near surface of the pin and the bush used for the conventional chain type wear testing (5% Nital etching). (Online version in color.)

Table 6. Comparison of testing condition.

Items		Newly developed wear testing	Conventional chain type wear testing
Idling time per one cycle		0.6 [sec]	5.1 [sec]
Definition of one cycle	N	Reciprocation	Revolving
Load	Pc	29 500 [N]	
Average sliding speed	V	2.19 [m/min]	
Sliding angle	θ_0	32.7 [degree]	
Condition of sliding surface		Dry	

© 2020 ISIJ

clarify the difference due to the testing method, the sliding surface is degreased to exclude the disturbance factors of the lubrication. Since the preliminary testing confirmed that the result variation is smaller, three number of tests are conducted for the newly developed wear testing. For the conventional chain type wear testing to be compared, two number of tests are conducted. For the conventional chain type wear testing, one cycle N can be defined when the chain is going around. Instead, for the newly developed wear testing machine, one cycle N can be defined as one reciprocating motion of the bush. Real roller chains are used with the number of cycles $N \geq 25 \times 10^4$ per year. In this study, therefore, $N = 25 \times 10^4$ is defined as the standard number of cycle N per year without considering idling time.

The total wear amount W_T can be defined as $W_T = W_P + W_B$ where W_P is the pin wear depth and W_B is the bush wear depth. This is because $W_T = W_P + W_B$ is related to the chain elongation. In the newly developed wear testing machine, W_T can be measured from the displacement amount of the hydraulic cylinder. In the conventional chain type wear testing machine, W_T can be measured from the total length change of the roller chain. Those measuring can be conveniently used without removing the test piece during the test.

4.2. Results of Wear Testing

Figure 13 and **Table 7** compare the wear amount $W_T = W_P + W_B$ for the number of cycle N. Here, W_T^N is the wear amount of the newly developed wear testing, and W_T^C

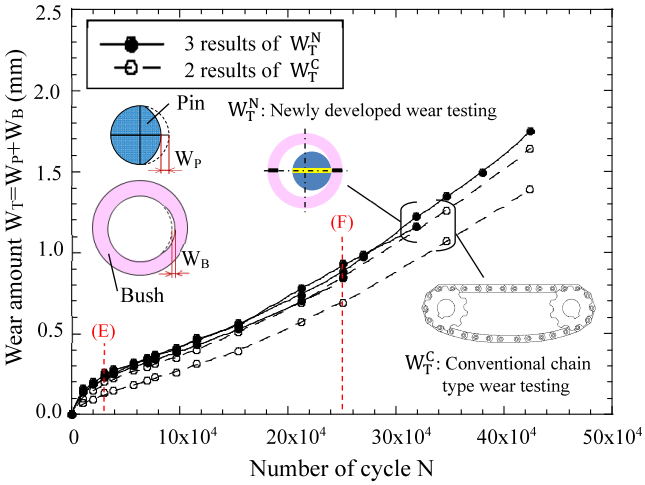

Fig. 13. Comparison of the wear amount between W_T^N (newly developed) and W_T^C (conventional). (Online version in color.)

Table 7. Definition and comparison between wear amount W_T^N and W_T^C measured from the displacement amount of the hydraulic cylinder for W_T^N, and from the chain elongation for W_T^C.

$$W_T^N\big|_k = \sum W_T^N / 3 = (\text{No. } 1 + \text{No. } 2 + \text{No. } 3)/3$$

$$\Delta W_T^N = W_T^N\big|_{k+1} - W_T^N\big|_k$$

$$W_T^C\big|_k = \sum W_T^C / 2 = (\text{No. } 1 + \text{No. } 2)/2$$

$$\Delta W_T^C = W_T^C\big|_{k+1} - W_T^C\big|_k$$

k	Number of cycle N ($\times 10^4$)	Wear amount $W_T = W_P + W_B$ [mm]								
		W_T^N: Newly developed wear testing					W_T^C: Conventional chain type wear testing			
		No. 1	No. 2	No. 3	$W_T^N\big\|_k$	ΔW_T^N	No. 1	No. 2	$W_T^C\big\|_k$	ΔW_T^C
1	1.0	0.14	0.16	0.14	0.147	0.147	0.10	0.07	0.085	0.085
2	2.0	0.19	0.20	0.19	0.193	0.046	0.15	0.09	0.120	0.035
3	3.0	0.24	0.26	0.23	0.243	0.050	0.20	0.13	0.165	0.045
4	3.9	0.26	0.28	0.25	0.263	0.020	0.22	0.15	0.185	0.020
5	5.8	0.32	0.31	0.30	0.310	0.047	0.27	0.18	0.225	0.040
6	7.0	0.35	0.34	0.32	0.337	0.027	0.29	0.21	0.250	0.025
7	7.7	0.37	0.36	0.34	0.357	0.020	0.31	0.23	0.270	0.020
8	9.6	0.41	0.40	0.38	0.397	0.040	0.35	0.26	0.305	0.035
9	12.0	0.46	0.47	0.43	0.453	0.056	0.40	0.31	0.355	0.050
10	15.0	0.56	0.55	0.53	0.547	0.094	0.51	0.39	0.450	0.095
11	21.0	0.74	0.78	0.70	0.740	0.193	0.69	0.57	0.630	0.180
12	25.0	0.88	0.93	0.85	0.887	0.147	0.84	0.69	0.765	0.135
–	27.0	0.97	0.99	–	0.980	–	–	–	–	–
–	32.0	1.22	1.16	–	1.190	–	–	–	–	–
13	35.0	1.35	–	–	1.350	0.463	1.26	1.07	1.165	0.400
–	38.0	1.50	–	–	1.500	–	–	–	–	–
14	42.0	1.75	–	–	1.750	0.400	1.64	1.39	1.515	0.350

© 2020 ISIJ

is the wear amount of the conventional chain type wear testing. At the standard number of cycle N = 25 × 10^4 denoted by point (F) in Fig. 13, W_T^N = 0.85–0.93 mm, and W_T^C = 0.69–0.84 mm. From the wear curves in both testing, both wear rates at the initial stage of the test are larger, and then the slopes remain almost constant, and the slopes slightly increase after the wear amount become larger than about 1 mm. Large amount of wear at the initial stage of the test is called as initial wear condition. This state lasts until the number of cycles about N = 3 × 10^4 denoted by point (E) in Fig. 13, and then changes to stable wear condition. Such a transition phenomenon is generally confirmed in adhesive wear of metals with repetition.[16,17]

Focusing on the variation in the wear amount due to the number of tests at N = 3 × 10^4 denoted by point (E) in Fig. 13, the variation is 0.03 mm for W_T^N and 0.07 mm for W_T^C. Similarly, at N = 25 × 10^4 denoted by pint (F) in Fig. 13, the variation is 0.08 mm for W_T^N and 0.15 mm for W_T^C. Thus, the variation of W_T^N is about half of the variation of W_T^C. This is consistent with the design principle of this new testing. The stable wear amount will be discussed in section 5.1.

5. Comparison of the Results between the Newly Developed Wear Testing and the Conventional Chain Type Wear Testing

5.1. Comparison of Wear Rate between the Newly Developed Wear Testing and the Conventional Chain Type Wear Testing under Stable Condition

The allowable wear amount in a real chain is usually 3 mm for the pin diameter D_P = 15.8 mm. Then, the initial wear amount $W_T^N|_k$ = 0.24 mm is only 8% of the allowable wear amount for the newly developed wear testing. And the initial wear amounts $W_T^C|_k$ = 0.17 mm is only 6% of the allowable wear amount for the conventional chain type wear testing. In other words, more than 90% of allowable wear amount are consumed under the stable wear condition. Therefore, stable wear amounts should be compared between the newly developed wear testing and the conventional chain type wear testing. First of all, wear rate is discussed.

The wear rate dW_T/dN can be determined from the amount of wear per cycle number denoted by dW_T^N/dN for the newly developed wear testing and dW_T^C/dN for the conventional wear testing. They can be obtained from Eqs. (1) and (2). The average amount of wear ΔW_T^N, ΔW_T^C in Table 7 is used for both testing.

$$\frac{dW_T^N}{dN} \cong \frac{\Delta W_T^N}{\Delta N},\ \Delta W_T^N = W_T^N|_{k+1} - W_T^N|_k \text{ in Table 7} \quad \cdots (1)$$

$$\frac{dW_T^C}{dN} \cong \frac{\Delta W_T^C}{\Delta N},\ \Delta W_T^C = W_T^C|_{k+1} - W_T^C|_k \text{ in Table 7} \quad \cdots (2)$$

As an example, Table 7 shows ΔW_T^N = 0.147 mm during the number of cycle N = 21 × 10^4 ~ 25 × 10^4. Then, from Eq. (1), the wear rate dW_T^N/dN = 3.68 × 10^{-6} mm/cycle can be obtained.

$$\frac{dW_T^N}{dN} \cong \frac{\Delta W_T^N}{\Delta N} = \frac{0.147}{25\times10^4 - 21\times10^4} = 3.68\times10^{-6}\,\text{mm/cycle}$$

Figure 14 shows the wear rates of both testing calculated using Eqs. (1) and (2). In Fig. 14, the number of cycle N is plotted as the median value of the measurement interval. For example, the result during the number of cycle N = 21 × 10^4 ~ 25 × 10^4 is plotted as the result at N = 23 × 10^4. The wear rate difference between dW_T^N/dN and dW_T^C/dN is significant under initial wear condition during N ≤ 3 × 10^4 whose number is denoted by point (G) in Fig. 14. However, then they are nearly the same under stable wear condition during N ≥ 3 × 10^4.

Let's consider why the wear rates dW_T^N/dN and dW_T^C/dN are different at the initial stage. It should be noted that the surface properties affect the initial wear of the pin and the bush. As shown in Fig. 11, at the near surface for dW_T^N/dN a lathe turning mark is observed but the oxide film is not observed. On the other hand, as shown in Fig. 12, at the near surface for dW_T^C/dN, an oxide film having a thickness of about 20 μm can be observed. In dry friction, since the oxide film on the metal surface prevents metal-to-metal contact, the friction and wear rate become smaller.[18–20] This is the reason why dW_T^N/dN is larger than dW_T^C/dN at the initial stage of the test. Since the thin oxide film often disappears at the initial stage of tests, the variation for dW_T^C/dN is always larger than the variation of dW_T^N/dN. During the pin and the bush reciprocating sliding motion under dry friction, the wear debris are attached at the sliding surface and the metal-to-metal contact area decreases. Therefore, the influence of the initial surface condition becomes smaller under the stable wear condition, the difference between dW_T^N/dN and dW_T^C/dN becomes smaller within 15%. From Fig. 14, the number of cycle N ≥ 3 × 10^4 corresponds to the stable wear condition where $W_T^N|_k \geq 0.24$ mm as shown in Table 7.

After the test finished, the pin and the bush were removed from the testing machine to measure the wear amount directly. **Table 8** shows the total wear amount W_T which can be defined as $W_T = W_P + W_B$ where W_P is the pin wear depth and W_B is the bush wear depth. The test piece No. 1 is measured for the newly developed wear testing and the test piece No. 2 is measured for the conventional wear testing. It should be noted that the ratio of the pin wear depth W_P to the total wear amount W_T is the nearly same for W_T^N and W_T^C, that is, $W_P/W_T^N \cong W_P/W_T^C$. The previous section

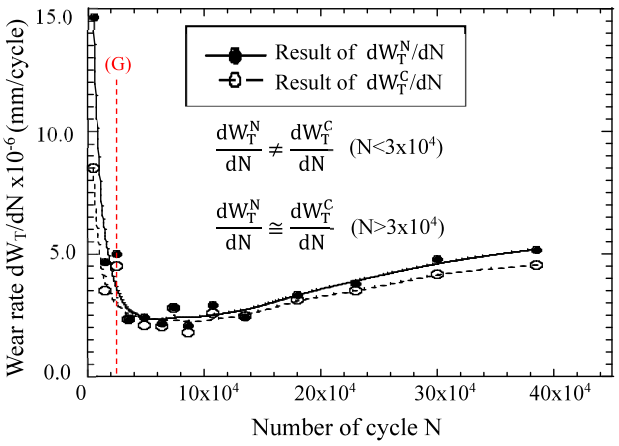

Fig. 14. Comparison of the wear rate between dW_T^N/dN (newly developed) and dW_T^C/dN (conventional). (Online version in color.)

© 2020 ISIJ

Table 8. Total wear amount $W_T^N \neq W_T^C$ and wear ratio $W_P/W_T^N = W_P/W_T^C$ directly measured wear amount in comparison with W_T^N and W_T^C in Table 7.

Items	W_T^N: Newly developed wear testing fom No. 1			W_T^C: Conventional chain type wear testing from No. 2		
Directly measured from the pin and the bush [mm]	W_P/W_T^N	0.46	$W_P=0.82$	W_P/W_T^C	0.45	$W_P=0.64$
	W_B/W_T^N	0.54	$W_B=0.95$	W_B/W_T^C	0.55	$W_B=0.79$
	$(W_P+W_B)/W_T^N$	1.0	$W_P+W_B=1.77$	$(W_P+W_B)/W_T^C$	1.0	$W_P+W_B=1.43$
Displacement amount of the hydraulic cylinder for W_T^N and Chain elongation for W_T^C from Table 7 [mm]	$W_T^N=1.75$			$W_T^C=1.39$		

describes that the total wear rates dW_T^N/dN and dW_T^C/dN are also the same under stable wear condition. The wear amount ratio for the pin and the bush is also the same for both testing. The wear amount W_T^N can be simply measured from the displacement amount of the hydraulic cylinder and the wear amount W_T^C can be simply measured from the chain elongation for W_T^C in Table 7. Those amounts W_T^N and W_T^C are in good agreement with the wear amount W_T directly measured from the pin and the bush in Table 8. Those results show that the wear amount can be evaluated accurately without removing the test piece.

5.2. Comparison of Cross-section Shape between the Newly Developed Wear Testing and the Conventional Chain Type Wear Testing

Figure 15(a) shows the cross-section change of the pin due to the newly developed wear testing. The crescent-moon-shaped wear range is symmetric to the x-axis. Figure 15(b) shows the cross-section change of the pin due to the conventional chain type wear testing. The crescent-moon-shaped wear range is approximately symmetric to the x-axis. Figure 15 shows similar wear shape can be obtained by the newly developed machine.

Figure 16(a) shows the cross-section change of the bush due to the newly developed wear testing. The wear shape is a crescent moon but the most wear position is situated at about −15° to the x-axis. Figure 16(b) shows the cross-section change of the bush due to the conventional chain type wear testing. The wear shape is a crescent moon but the most wear position is situated at about −15° to the x-axis. The asymmetric wear shape to the x-axis may be due to the influence of the sprocket engaging. Figure 16 shows similar wear shape can be obtained by the newly developed machine. Although the sliding angle between the pin and the bush is $\theta_0=32.7°$ as described in section 4.1 for the testing condition, the wear can be seen more widely about 180°as shown in Figs. 15 and 16. This is because the contact area and the radius of curvature at the contact surface increase with increasing the wear amount. Since the wear shapes of the pins and bushes are nearly the same, the newly developed wear testing machine has sufficient reproducibility of real roller chains.

5.3. Comparison of Wear Surface Condition between the Newly Developed Wear Testing and the Conventional Chain Type Wear Testing

Figure 17 compares the wear surface condition of the pin. Figure 17(a) shows the pin surface after the newly developed wear testing and Fig. 17(b) shows the pin surface

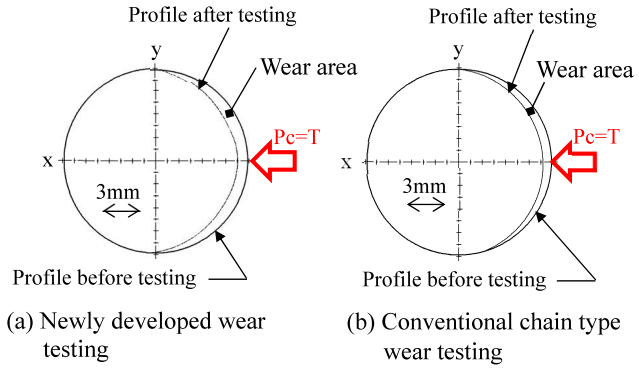

Fig. 15. Pin diameter profile change before and after testing. (Online version in color.)

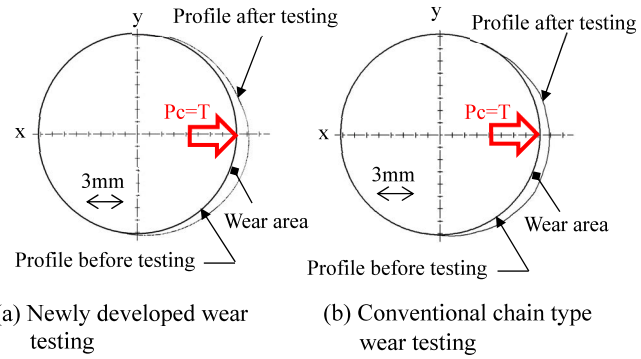

Fig. 16. Bush inside diameter profile change before and after testing. (Online version in color.)

after the conventional chain type wear testing. The sliding direction is perpendicular to the pin axis as shown in Fig. 17. Figures 17(a-2) and 17(b-2) show typical groove-like scratches and Figs. 17(a-3) and 17(b-3) show the typical adhesive surface where the black material is attached. Those macroscopic observations show that most of pin surfaces in Figs. 17(a) and 17(b) are dominated by scratches or adhesive surface in a similar way.

Figure 18 compares the wear surface of the bush. Figure 18(a) shows the bush surface after the newly developed wear testing and Fig. 18(b) shows the bush surface after the conventional chain type wear testing. The sliding direction is perpendicular to the pin axis as shown in Fig. 18. Figures 18(a-2) and 18(b-2) show groove-like scratches observed. Scratches of the conventional testing are finer than scratches of the new testing. And the surface of the conventional testing is less shiny than the surface of the new testing. Figures 18(a-3) and 18(b-3) show the typical adhesive surface where the black material is attached. The

© 2020 ISIJ

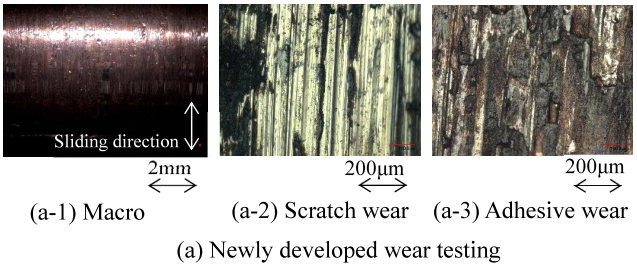

Fig. 17. Wear surface of the pin. (Online version in color.)

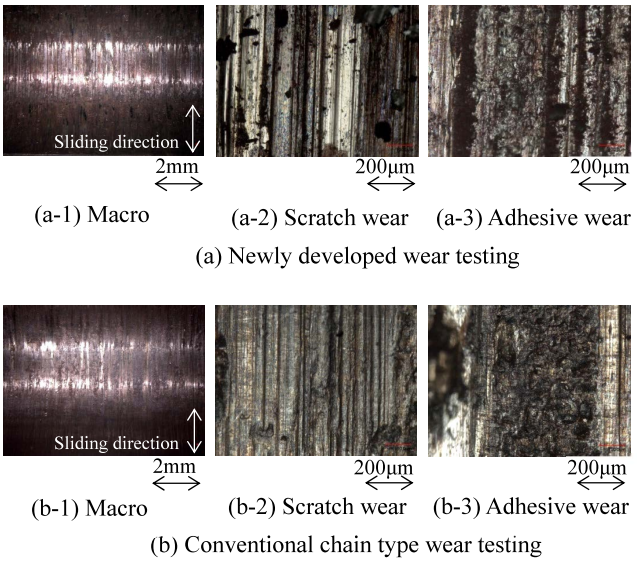

Fig. 18. Wear surface of the bush. (Online version in color.)

difference of the wear surface of the bush is caused by the difference of the sliding condition. The sliding state between the pin and the bush is always under compression during the test for the newly developed wear testing, but there is a period without compression for the conventional chain type wear testing as shown in Table 1. Moreover, as shown in Table 6, the idling time between the reciprocating motion is different. Those differences of no compression and idling time may affect the wear surface of the bush. However, the effect is not very large since the wear amount ratio of the pin and the bush is almost the same as shown in Table 8 and similar wear surfaces can be observed.

6. Conclusion

To evaluate the wear resistance of the roller chain, huge amount of time and cost were spent by using the conventional wear testing machine. This study therefore focused on developing a new wear testing machine composed by minimum components to simplify the wear testing. The conclusions can be summarized in the following way.

(1) By using the newly developed wear testing machine, the wear amount can be evaluated conveniently without using main chain components such as inner plate, outer plate and roller. The wear testing variation is smaller than the variation of the conventional chain type wear testing.

(2) Wear mechanism of the real roller chain was clarified in the real roller chain during operation. The wear of the roller chain occurs when the bend angle is changed under the tensile load. In the driving state, the pin is fixed under the compressive state, and the bush rotates. In the driven state, the bush is fixed under the compressive state, and the pin rotates (see Figs. 4 and 5).

(3) The newly developed wear testing machine was developed by considering the sliding state between the pin and the bush of the real roller chain. The newly developed wear testing machine consists of only two parts, that is, the pin and the bush to improve the reproducibility, to reduce the cost of test pieces, to reduce the preparing time, and to be controlled easily (see Figs. 6 and 7).

(4) The results show that the wear rate and the wear status are almost the same between the newly developed wear testing machine and the conventional chain type wear testing machine under stable wear condition. Therefore, the newly developed wear testing machine has sufficient reproducibility with high accuracy compared to the conventional chain type wear testing machine.

REFERENCES

1) T. Yasuda: *J. Jpn. Soc. Lubr. Eng.*, **10** (1965), 525 (in Japanese).
2) G. Rozing, V. Alar and V. Marusic: *Interdiscip. Descr. Complex Syst.*, **13** (2015), 461.
3) J. D. Bressan, D. P. Daros, A. Sokolowski, R. A. Mesquita and C. A. Barbosa: *J. Mater. Process. Technol.*, **205** (2008), 353.
4) Y. Zhang, Z. Yang and D. Li: *Proc. Inst. Mech. Eng., Part J*, **233** (2019), 927.
5) P. Thongjitr, P. Ninpetch and P. Kowitwarangkul: *Mater. Today: Proc.*, **5** (2018), 9431.
6) C. Kim, J. Chung and J. Song: *Adv. Mech. Eng.*, **9** (2017), No. 1. https://doi.org/10.1177/1687814017723296
7) S. Xu, Y. Wang and F. Meng: *Proc. Inst. Mech. Eng., Part C*, **220** (2006), 1569.
8) H. Peeken and W. Coenen: *Wear*, **108** (1986), 303.
9) C. A. Brockley: *Wear*, **4** (1961), 333.
10) S. J. Radcliffe: *Tribol. Int.*, **14** (1981), 263.
11) N. E. Hollingworth: *Tribol. Int.*, **20** (1987), 3.
12) S. Noguchi, H. Yoshiba, S. Nakayama and T. Kanada: *J. Adv. Mech. Des. Syst. Manuf.*, **3** (2009), 355.
13) S. C. Burgess, T. Pyper and C. S. Ling: *Proc. Inst. Mech. Eng., Part C.*, **227** (2013), 1047.
14) D. C. Oscar and A. S. Arthur: Chain Feed Mechanism for an Induction Heating Furnace, U. S. Patent US4582972A, (1986).
15) M. Nakagome: Safety Design of Roller Chains, Yokendo, Tokyo, (1989), 101 (in Japanese).
16) K. Hiratsuka: *Trans. Jpn. Soc. Mech. Eng. C*, **58** (1992), 3362 (in Japanese).
17) Y. Amamoto and H. Goto: *Tribol. Int.*, **39** (2006), 756.
18) M. Satoyoshi and F. Hayama: *J. Jpn. Inst. Met.*, **32** (1968), 11 (in Japanese).
19) H. Kato: *Tribol. Int.*, **41** (2008), 735.
20) H. Kato: *Wear*, **255** (2003), 426.

Appendix: Reproducibility of Sliding Direction for the Pin and the Bush

In this appendix, the details of the sliding directions of the pin and the bush will be discussed. In the real roller chain, **Figs. A1**(a) and A1(b) illustrate the sliding direction focusing on the pin and the bush from Figs. 5(a) and 5(b). Figures A1(a-1)–A1(a-3) are corresponding to Figs.

© 2020 ISIJ

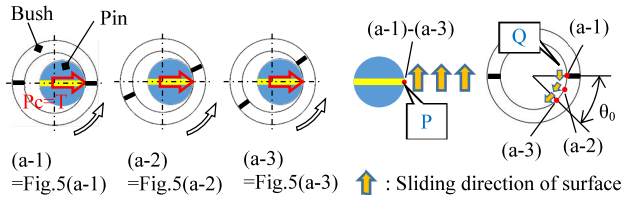

(a) Sprocket driving state causing uni-directional friction for Bush

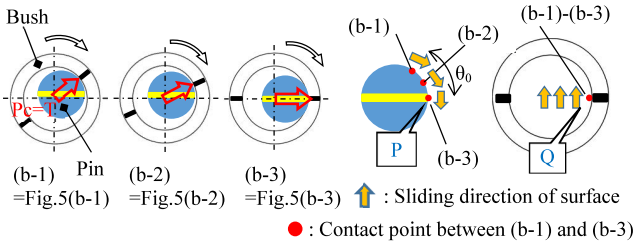

(b) Sprocket driven state causing uni-directional friction for Pin

Fig. A1. Real roller chain under uni-directional friction between the driving state and the driven state. (Online version in color.)

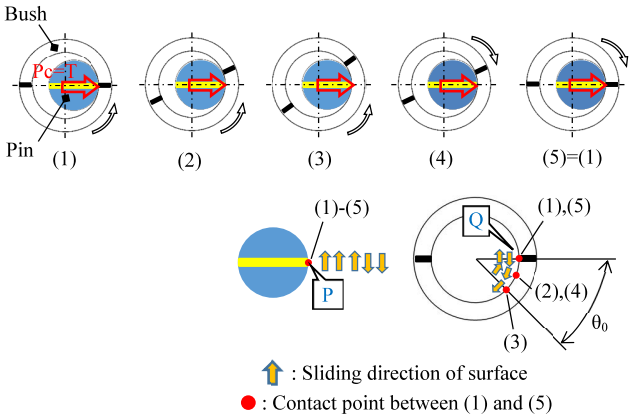

Fig. A2. Newly developed wear testing machine under reciprocating friction for 1 cycle. (Online version in color.)

5(a-1)–5(a-3), and A1(b-1)–A1(b-3) are corresponding to Figs. 5(b-1)–5(b-3). Although in Fig. 5(b) the loading direction is fixed, in Fig. A1(b) the position of the pin is fixed.

First of all, the contact point change is explained in relation to the sliding direction change between the pin and the bush. As shown in Fig. A1(a), in the driving state, the pin is fixed under the compressive contact load Pc = T, and the bush rotates from $\theta_A=0$ to $\theta_A=\theta_0$. Therefore, the contact point of the bush varies in the range of angle $\theta_A=0\sim\theta_0$ under the fixed contact point of the pin. As shown in Fig. A1(b), in the driven state, the bush is fixed under the compressive contact load Pc = T, and the pin rotates from $\theta_A=0$ to $\theta_A=\theta_0$. Therefore, the contact point of the pin varies in the range of angle $\theta_A=0\sim\theta_0$ under the fixed contact point of the bush.

Next, let's focus on the contact points P and Q whose locations may affect the chain elongation. In the real roller chain, the sliding direction of point P on the pin surface is perpendicularly upward in Fig. A1(a) and perpendicularly downward in Fig. A1(b-3). The sliding direction of point Q on the bush surface is perpendicularly downward in Fig. A1(a-1) and is perpendicularly upward in Fig. A1(b). In other words, the sliding motions of the points P and Q are reciprocating.

In the newly developed wear testing machine, **Fig. A2** illustrates the sliding direction for the pin and the bush during operation. As shown in Fig. A2, the pin is fixed under the compressive contact load Pc = T, and the bush rotates in clockwise and counterclockwise directions in the range from $\theta_A=0$ to $\theta_A=\theta_0$. During the operation, the sliding motions of the point P and Q are reciprocating. Since the sliding direction during the operation is the same as the sliding direction of the real roller chain, the newly developed wear testing machine adopts such reciprocating motions.

© 2020 ISIJ